J Biol Phys (2013) 39:173–181
DOI 10.1007/s10867-013-9304-1

SHORT NOTES

Evolution of nanoparticle-induced distortion on viral polyhedra

Sumistha Das · Alokmay Datta · Smita Mukherjee · Nupur Biswas · Arunava Goswami

Received: 12 December 2012 / Accepted: 7 February 2013 / Published online: 9 March 2013

Abstract Morphological changes in the polyhedra of the *Bombyx mori* L. nuclear polyhedrosis virus (BmNPV), a baculovirus causing the deadly grasserie disease in silkworms, brought about by mixing with lipophilically capped amorphous silica nanoparticles (LASN, average size 10 ± 2 nm) were studied with scanning electron microscopy (SEM) and Fourier transform infrared (FTIR) spectroscopy. SEM shows that the regular octagonal polyhedra facets are replaced by a larger number of newly formed irregular ones. The average number of facets reveals a nonlinear growth pattern with nanoparticle (NP) concentration, where an initial linear region ends in a plateau. IR bands corresponding to vibration modes of the capping show (a) a saturation of the area under the band with NP concentration, indicating a correlation with attachment to viral polyhedra and (b) a narrowing of the band per NP from the linear to the plateau portions of the distortion curve, suggesting non-equilibrium and equilibrium situations, respectively.

Keywords Silica nanoparticle · Baculovirus polyhedra · Morphological deformity · Boltzmann equation

1 Introduction

Nanoparticles (NPs) are not only characterized by their size but by the fact that they are nano-sized pieces of some material that is naturally found in bulk. Compared to the bulk, NPs are inherently unstable due to their immense surface-to-volume ratio and the

S. Das (✉) · A. Goswami
Biological Sciences Division, Indian Statistical Institute,
203, B. T. Road, Kolkata 700108, India
e-mail: sumistha.das@gmail.com

A. Datta · S. Mukherjee · N. Biswas
Applied Material Science Division, Saha Institute of Nuclear Physics,
1/AF, Bidhannagar, Kolkata 700064, India

consequent high surface free energy [1]. NPs have played a major role in biological systems due to this high surface free energy that leads to their exceptional interactive capacity [2].

In our previous communications, we investigated a particular instance of such nano-bio interactions between amorphous silica nanoparticles and viruses. Specifically, we have studied the distortions induced by amorphous nano-silicates (ANS) and lipophilically coated amorphous silica nanoparticles (LASN) on the polyhedra of *Bombyx mori* nuclear polyhedrosis virus (BmNPV), and the specific bio-functionality emerging from these distortions [3, 4]. BmNPV causes enormous damage to silkworm industry through its mediation of the grasserie disease in the *Bombyx mori* silkworm larvae resulting in 100% mortality [5]. During replicative cycle of the virus, two virion phenotypes are produced. One virion type, called polyhedra-derived virus (PDV), is embedded in an electron-dense crystalline protein matrix called polyhedron/occlusion body leading to nomenclature nuclear poyhedrosis virus [6–8]. Polyhedra bodies are polyhedral in shape, composed majorly of polyhedrin protein [9] and contain numerous virions. A second phenotype budded virion (BV) is generated during the early phase of infection. PDVs are highly infectious to midgut columnar epithelial cells and are accountable for the horizontal transmission of the virus from insects-to-insects through polyhedra bodies. We found that LASN causes a significant reduction in mortality of BmNPV-infected silkworm larvae [3], and microscopic studies revealed that LASN also severely alters the structure of the virus envelope by a distortion of the viral polyhedra [10]. Again, we found that the ANS–virus complex led to both severe distortion in the viral polyhedra as well as substantial enhancement of longevity in the diseased silkworm larvae and $35 \pm 5.3\%$ larvae completed their lifecycle (i.e., formed normal pupae and enclosed as moth), whereas 100% larvae infected with BmNPV alone died within 36 h [4]. Hence, it became evident that the distorted polyhedra play a role in the reduction of mortality of the infected larvae.

In this communication, we have focused on a detailed Scanning electron microscopy (SEM) of the evolution of this distortion with NP concentration, with a future goal of understanding qualitatively and quantitatively the underlying polyhedra-NP interactions and correlating them with bio-functionality. We have also carried out Fourier transform infrared (FTIR) spectroscopy of the system to investigate how the virus-NP bonding changes with NP concentration.

The structure of the paper is as follows: after this introductory section, we have sections dealing with the NPs used, the viral polyhedra, and the interaction of the nanoparticles with them, ending finally with a concluding section and an outlook.

2 Experimental

2.1 Materials

Chemicals such as tetra-methyl-orthosilicate (TMOS), 3-mercaptopropyl-trimethoxysilane (MPTS) were purchased from Merck (Darmstadt, Germany). All other chemicals used were of reagent grade and available locally. Chemicals were used without further purification.

2.2 Synthesis of NP

Nanosilica was prepared from TMOS via sol–gel method and was surface functionalized with MPTS. Methanolic solution of TMOS and 50% aqueous methanol solution were

prepared separately. These two solutions were mixed drop-wise with strong agitation and kept under reflux conditions (around 67 °C) with a final ratio of TMOS: water: methanol being 1:4:12. Once the nanosilica cores were prepared, a solution of MPTS in methanol was added drop-wise with vigorous agitation to produce the thiol-capped nanosilicas. This suspension was kept under reflux conditions for 1–2 h. The ratio of TMOS:MPTS:water:methanol was maintained at 1:1:4:15. The lipophilic nanosilica was purified by vacuum filtration, washed several times with double distilled water and finally dried to powder form.

2.3 Physical characterization of NP

LASN was subjected to different microscopic techniques for physical characterization. During SEM (FEI Quanta 200, FEI Inc., USA) studies, alcoholic suspension of LASN was smeared on 1 cm × 1 cm clean glass slides and air-dried. Each slide was coated with gold-palladium at 5 mA by SC7620 sputter coater. For TEM (JEM 2010, Jeol Inc., USA) studies, 15 µl NP suspension was deposited on copper grid (Pro Sci Tech Inc., Australia. 300 mesh) under laminar hood and was allowed to air dry. During both SEM and TEM studies, the samples were dispersed by ultrasonication.

2.4 Viral polyhedra

Cohesion at the polyhedral edges was expected to be less than that at the faces. Hence, any change in the surface energy of the polyhedra would affect the edges the most and we hypothesized that alteration of the surface energy by NPs may initiate a 'roughening' transition that would smoothen the edges. This prompted us to extract the polyhedra and to characterize them before subjecting them to the LASN.

2.4.1 Isolation of BmNPV polyhedra

Prolegs of BmNPV infected (36 h post infection) Nistari strain of silkworm larvae (*B. mori)* were punctured and hemolymph was collected in the presence of phenyl-thio-urea (3 mM) to avoid melanization [11]. Polyhedra bodies or occlusion bodies (OBs) were centrifuged at 20,000 × g for 1 h and the pellet was washed three times with distilled water until the supernatant was devoid of any turbidity of floating lipid. Pellets were re-suspended in 0.5% sodium dodecyl sulphate (1 ml per insect equivalent) by homogenization to disrupt the polyhedra aggregates. The polyhedra suspension was again pelleted at 20,000 × g for 1 h and re-suspended in Tris-EDTA buffer (0.5 ml/insect equiv). The purified OBs were suspended in 3 ml of deionized water and its O.D. value was measured at 550 nm in an UV-visible spectrometer (Perkin Elmer Lambda 25). 1.0 $O.D._{550}$ was equal to 0.35 mg/ml OB concentration where 1 mg equals to about 2×10^6 polyhedra.

2.4.2 BmNPV polyhedra-NP complex incubation

Viral morphology with and without LASN treatment was elucidated following SEM [12, 13] with minor modifications in the protocol. First, 0.5 mg of dry NP powder was added in 1.5 ml of ethanol and made an ethanolic solution of LASN. In one aliquot, the ethanolic solution of LASN was mixed at a 1:1 ratio with polyhedra stock solution, and vortexed for 5 min for proper mixing and kept undisturbed at room temperature for 3 h. Then both the solutions (with and without NPs) were directly seeded on to 1 cm × 1 cm xylene cleaned

glass slides and allowed to air dry. Then the slides were coated with gold-palladium at 5 mA by SC7620 sputter coater and the samples were analyzed by SEM. The final concentrations of NPs used were 250, 500, 1,000, 2,000, 4,000, and 7,000 μg/ml. Image analysis of SEM micrographs was done using ImageJ freeware of National Institute of Health, USA.

2.4.3 FT-IR spectroscopy of polyhedra-LASN complex

One hundred μl of stock viral suspension was diluted with 100 μl of deionized water and 50 μl of alcoholic NP solution was added on it. Control was prepared using alcohol. Five different NP concentrations, 500, 1,000, 2,000, 4,000 and 7,000 μg/ml were considered as treatments. All the viral suspensions were incubated for 3 h with occasional shaking; 5 μl of each suspension was drop cast on a zinc selenide (ZnSe) plate, air dried for 24 h, and spectra were taken subsequently in the 700 cm^{-1} to 1,300 cm^{-1} range in transmission mode of a Perkin Elmer spectrum 400 (Massachusetts, USA) instrument.

3 Experimental results and discussion

3.1 Physical characterization of NP

SEM (Fig. 1a) and TEM (Fig. 1b) studies revealed that the average size of the synthesized LASN is 10 ± 2 nm with a log-normal distribution, as shown by the solid line fitting the centers of the bars in the bar graph of Fig. 1c, obtained from TEM. Several TEM images of the particles were taken and the average size of the particles was determined by measuring the size of around 200 particles.

3.2 Scanning electron microscopy of BmNPV polyhedra–nanoparticle complex

SEM images (Fig. 2) represent the most striking evidence of the regularity of the pristine polyhedra and its damage caused by NPs. Figure 2a shows a pristine polyhedra body with its near-perfect polygonal structure, sharp edges, and smooth walls, while Fig. 2b–d show the different stages of damage caused by LASN, as the concentration of the latter is increased. In Fig. 2b we see that the effect of even 500 μg/ml of LASN is negligible and the LASNs start affecting the polyhedra only after a concentration of 1,000 μg/ml is applied. However, once the process starts, it spreads rapidly as is evidenced in Fig. 2c where 2,000 μg/ml of LASN is used. The surface has become ragged and the edges roughened, leading to a

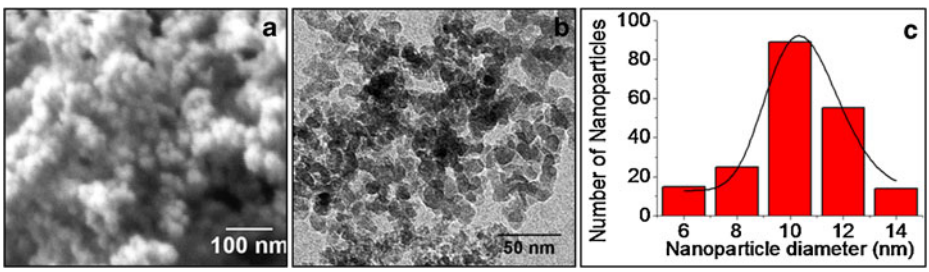

Fig. 1 Physical characterization of lipophilic amorphous silica nanoparticles (LASN). **a** Scanning electron micrograph and **b** transmission electron micrograph. **c** Size distribution from the TEM image

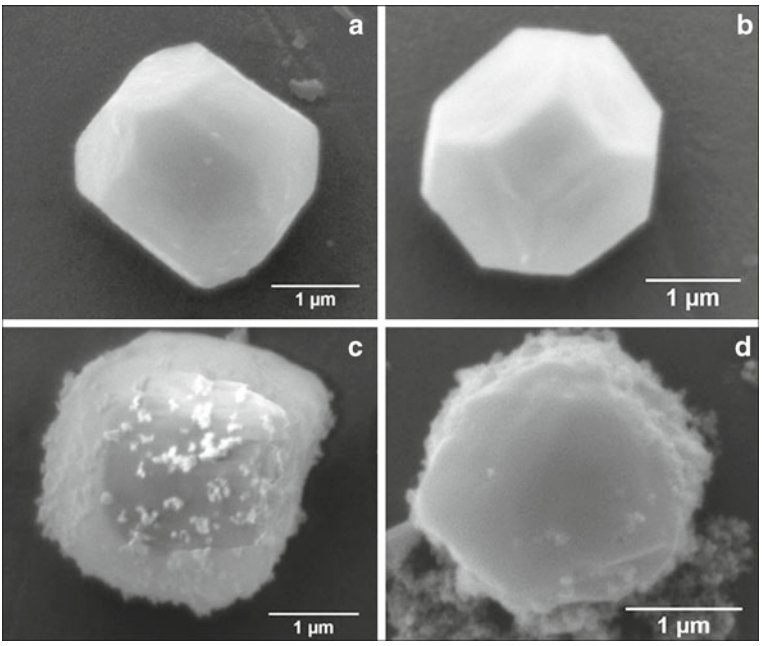

Fig. 2 Scanning electron micrographs showing the morphological evolution of a *Bombyx mori* nuclear polyhedrosis viral (BmNPV) polyhedra with increasing concentration of LASN. **a** Pristine viral polyhedra and polyhedra treated with **b** 500 μg/ml, **c** 2,000 μg/ml, **d** 7,000 μg/ml of LASN

general loss of the regular symmetry. This roughening also saturates quite rapidly and in Fig. 2d, with 7,000 μg/ml of LASN concentration we find the effect to be almost the same. The structure is approximately spherical confirming our hypothesis of roughening. It is to be noted, however, that the diameter remained the same, indicating absence of any swelling mechanism operating in the system. There is no clear evidence of deflation from this image, since SEM images are generally averaged over the normal to the focal plane and hence the vertical resolution of such images is very poor.

In order to quantify the roughening caused by LASN on viral polyhedra, we considered that the main action of roughening is to increase the number of facets of the polyhedra. Image analysis using the ImageJ freeware of the National Institutes of Health, USA, enabled us to determine the average number of facets (N) per LASN as a function of the LASN concentration c. This is shown in Fig. 3, where the qualitative features of the dependence of roughening on LASN concentration is borne out quantitatively. The observed data (open circles) fit beautifully to a Boltzmann curve (solid line) given by

$$N = N_f \exp(c/\Delta c) \,/ (1 + \exp(c/\Delta c)) \tag{1}$$

used often for mathematical modeling of growth in biological systems [14, 15]. Here N_f, the final number of facets, comes out to be 15.98 ± 0.09, i.e., ≈ 16, while the value of Δc, half of the difference in concentration over the linear growth region, shows the value 677.09 ± 25.80 μg/ml, consistent with direct observation. As the Boltzmann relation suggests, the rate of evolution of faceting with LASN concentration at any point consists of a positive part that depends linearly on the number of existing facets and a negative or self-limiting

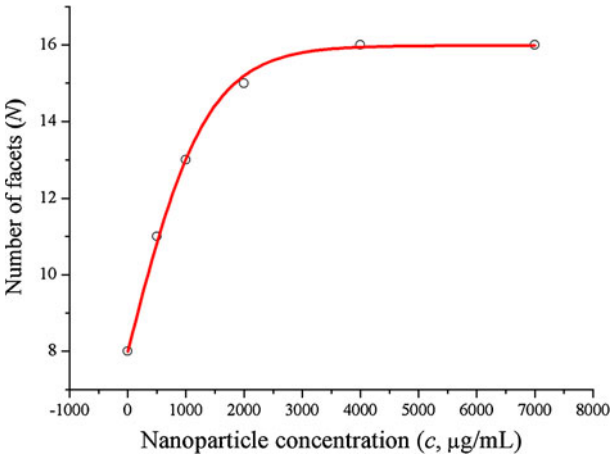

Fig. 3 Image analysis of NP induced viral deformation: graphical illustration on effect of LASN on the number of structural facets generated

part that has a quadratic dependence on this number. The results indicate that a steady-state condition was achieved by the system beyond a certain threshold concentration.

3.3 FT-IR analysis of BmNPV polyhedra–nanoparticle complex

In order to understand the molecular mechanism behind the distortion of the viral polyhedra by the LASNs, we carried out FTIR spectroscopy of the pristine and the NP-treated virus and the spectra of these in the 700 cm^{-1} to 1,300 cm^{-1} range, where we found the effect of the NP treatment to be most important, are shown in Fig. 4a–d. Whereas in the pristine sample (Fig. 4a) there are no strong peaks, a strong and broad band appears when 500, 2,000, and 7,000 μg/ml LASN are used, as shown in Fig. 4b–d, respectively. In our analysis, the individually resolved peaks are shown as Gaussian fits (purple) while the total band is fitted as a convolution (red) of these peaks. The two main peaks are found centered at 1,107 cm^{-1} and 1,212 cm^{-1} and are tentatively assigned to the symmetric (S_s) and asymmetric (S_a) stretching vibrational bands of C-Si-O, the bond between the silica core and the lipophilic capping of the LASN. This bond is expected to exist for most organic cappings of silica and silicate cores and thus these bands can serve as 'fingerprints' for this class of NPs.

We have shown the areas under the S_s peak (squares) and the S_a peak (circles) as functions of c, the LASN concentration in Fig. 5a. Both sets fit reasonably well to Boltzmann growth curves (solid lines). If we assume that the area under the peak varies with the number of NPs (n) giving rise to the peak, Fig. 5a shows that n saturates beyond $c \sim 4{,}000$ μg/ml, which signifies that n is not the *total* number of NPs but rather the number of NPs attached to the viral polyhedra, since it becomes independent of the concentration of NPs administered.

From the above result, it is clear that in order to follow the dynamics of attachment of LASNs to the polyhedra, we require to scale the widths of these peaks with n, which is proportional to the area under the peaks. If we name the peak width/peak area ratio as $\Delta\sigma$ and plot this quantity, in effect $\sim (\tau n)^{-1}$, τ being the lifetime in the corresponding vibrational state, as a function of c, we arrive at the curves in Fig. 5b, where data for the S_s

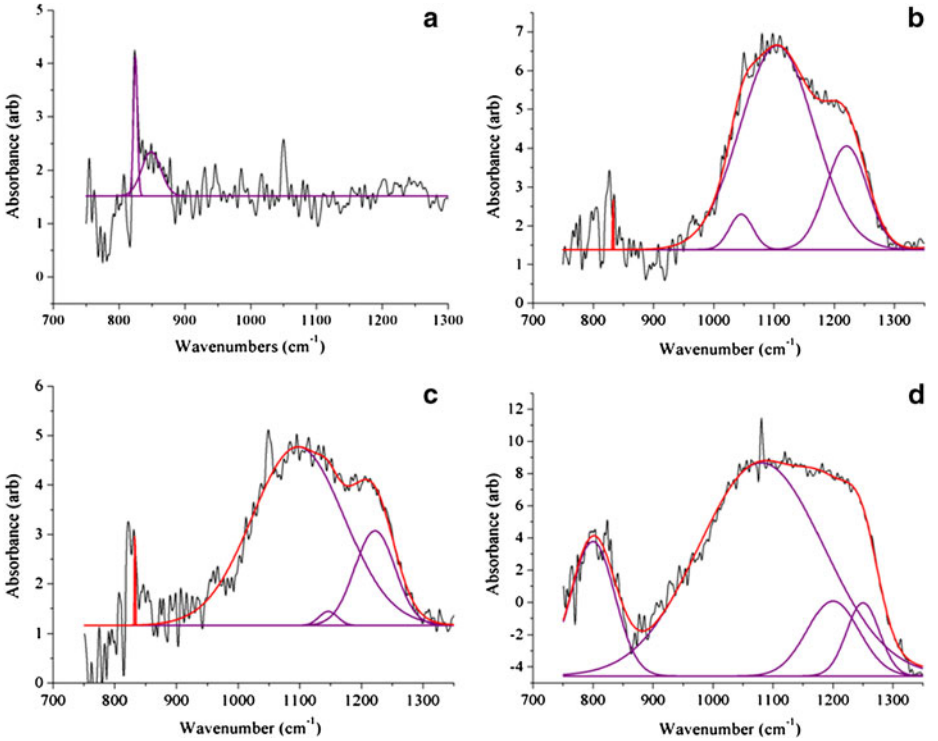

Fig. 4 Fourier transform-infrared (FT-IR) spectra showing the effect of LASN on BmNPV polyhedra. The individual peaks are fit with Gaussians (*purple lines*) while these are convoluted to fit the composite band (*red line*). The spectrum for pristine polyhedra is shown in **a** whereas spectra for polyhedra treated with 500 μg/ml, 2,000 μg/ml and 7,000 μg/ml LASN are shown in **b**, **c**, and **d**, respectively

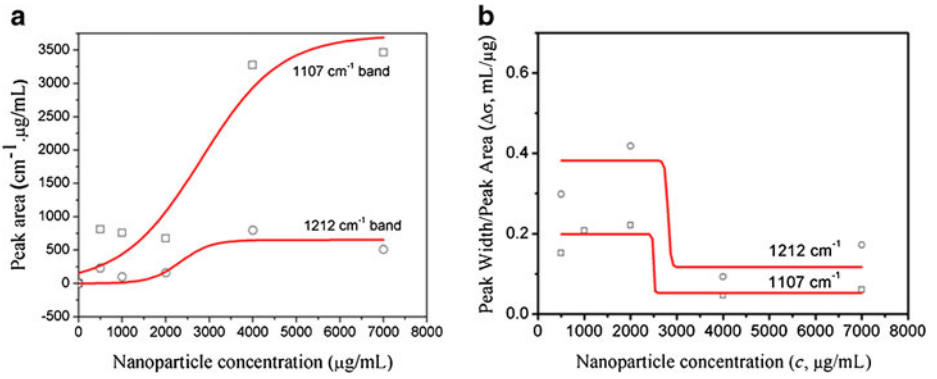

Fig. 5 Graphical relations between **a** peak area and LASN concentration **b** peak width/peak area and LASN concentration

peak are shown as squares while those for the S_a peak are shown as circles. The data again fit reasonably well to Boltzmann decay curves (solid lines) given by

$$\Delta\sigma = \Delta\sigma_f + \left(\Delta\sigma_i - \Delta\sigma_f\right) / \left(1 + \exp\left[(c - c_i)/\Delta c\right]\right) \quad (2)$$

where $\Delta\sigma_{i(f)}$ = initial (final) value of the peak width/peak area ratio, c_i = initial value of LASN concentration, and, as before, Δc = half the concentration difference over the linear decay region in both cases. For the S_s peak, the values of $\Delta\sigma_i \approx 0{\cdot}2$ ml/μg, $\Delta\sigma_f \approx$ 0.05 ml/μg, $c_i \approx$ 2,500 μg/ml, and $\Delta c \approx$ 66 μg/ml, whereas for the S_a peak these values are 0.4 ml/μg, 0.1 ml/μg, 2,800 μg/ml, and 66 μg/ml, respectively. Since the fits are not as good as in Fig. 3, the error bars are not provided here. The closeness of these values indicates the similarity in the dynamics and this, in turn, affirms that the assignment of the bands to similar degrees of freedom.

A drop in the value of $(\tau n)^{-1}$ signifies going to a vibrational state with a longer lifetime. We find that, in both the stretch modes, this value shows a fourfold drop as the LASN concentration goes above 3,000 μg/ml, indicating a commensurate gain in lifetime. Comparison of this result with the result of the previous section suggests that the steady-state condition in faceting or roughening of the viral polyhedra achieved by the LASN correlates strongly with a longer lifetime state of the C-Si-O stretch modes of the LASN attached to the polyhedra, whereas the dynamical state of roughening correlates with a shorter-lived state of these modes. This suggests that the molecular basis of the roughening observed in the mesoscopic length scales lies in achieving a 'long-living' state of the stretching of lipophilic capping layer of nanoparticles attached to the viral polyhedra, passing through a 'short-living' dynamical state. However, the exact mechanism of conversion of this stretching at molecular level to roughening at the level of micrometer length scales is yet to be elucidated and work towards that goal is underway.

4 Conclusions and outlook

We have studied the roughening of the polyhedra covering of BmNPV, which causes the dreaded *grasserie* disease in silkworm larvae, by LASN, which reduces the mortality caused by this disease, as a function of the NP concentration. We have also studied the effect of this concentration on NP capping-viral polyhedra bonding through infrared spectroscopy of the various vibrational modes. We found that both types of data point to a dynamical state and a steady state in corresponding concentration ranges—in the first a regime of fast increasing faceting ending in a state of constant number of facets, while in the second two modes of stretching vibration of the lipophilic coating attached to the polyhedra, both with a short-lived and a long-lived state. This strong correlation between events at widely different length scales—faceting at micrometer scales and stretching at sub-nanometer scales points to a hierarchy of dynamics at different length and time scales, as is expected for complex systems in general and bio-materials in particular [16].

The results obtained from this study help in the elucidation of the morphological changes induced on viral polyhedra by a specifically capped NP of a specific composition, which has already been shown to have a particular biological function [3]. This is a crucial step towards our goal of correlating this bio-functionality with the particularly prepared NP, which, in turn would serve to increase the efficacy of this particular NP in relation to that biological function, and more importantly, to provide a way to understand NP-virus interactions in

general. The major interest of this work lies in the fact that it connects the mechanical response of the viral polyhedra to NPs to the stability of the NP-polyhedra bonding.

Acknowledgements The authors would like to thank the Department of Biotechnology, Government of India, (grant nos- BT/PR9050/NNT/28/21/2007, BT/PR15217/NNT/28/506/2011 and BT/BIPP0439/11/10) and Indian Council of Agriculture Research (grant nos- NAIP/Comp-4/C3004/2008-09 and NFBSFARA/GB-2019/2011-12) for their financial support. Indian Statistical Institute (ISI) plan project for 2011–2012 was also used for funding this work. NB thanks the CSIR, New Delhi, for a senior research fellowship.

References

1. Charra, F., Gota-Goldmann, S.: Mesoscopic and nanostructured materials. In: Martienssen, W., Warlimont, H. (eds.) Springer Handbook of Condensed Matter and Materials Data, pp. 1031–1071. Springer, Berlin (2005)
2. Wang, X., Liu, L., Ramström, O., Yan, M.: Engineering nanomaterial surfaces for biomedical applications. Exp. Biol. Med. **234**, 1128–1139 (2009)
3. Rahman, A., Seth, D., Mukhopadhyaya, S.K., Brahmachary, R.L., Ulrichs, C., Goswami, A.: Surface functionalized amorphous nanosilica and microsilica with nanopores as promising tools in biomedicine. Naturwissenschaften **96**, 31–38 (2009)
4. Rahman A., Biswas, N., Ulrichs, C., Büttner, C., Bramhachary, R.L., Goswami, A., Datta, A.: Nanoparticle–virus complex shows enhanced immunological effect against baculovirus. J. Nanosci. Nanotechnol. **9**, 1–10 (2009)
5. Ponnuvel, K.M., Nakazawa, H., Furukawa, S., Asaoka, A., Ishibashi, J., Tanaka, H., Yamakawa, M.: A lipase isolated from the silkworm *Bombyx mori* shows antiviral activity against nucleopolyhedrovirus. J. Virol. **77**, 10725–10729 (2003)
6. Adams, J.R., McClintock, J.T.: Baculoviridae. Nuclear polyhedrosis viruses. Part 1. Nuclear polyhedrosis viruses of insects. In: Adams, J.R., Bonami, J.R. (eds.) Atlas of Invertebrate Viruses, pp. 89–180. CRC Press, Florida (1991)
7. Murphy, F.A., Fauquet, C.M., Bishop, D.H.L., Ghabrial, S.A., Jarvis, A.W., Martelli, G.P., Mayo, M.A., Summers, M.D. (eds.): Virus Taxonomy: Classification and Nomenclature of Viruses. Sixth Report of the International Committee on Taxonomy of Viruses, p. 586. Springer, New York (1995)
8. Blissard, G.W., Rohrmann, G.F.: Baculovirus diversity and molecular biology. Annu. Rev. Entomol. **35**, 127–155 (1990)
9. Hooft van Iddenkinge, B.J.L., Smith, G.E., Summers, M.D.: Nucleotide sequence of the polyhedrin gene of *Autographa californica* nuclear polyhedrosis virus. Virol. **131**, 561–565 (1983)
10. Biswas, N., Rahman, A., Datta, A., Goswami, A., Bramhachary, R.L.: Nanoparticle surface as activation site. J. Nanosci. Nanotechnol. **10**, 1–5 (2010)
11. Rahman, M., Gopinathan, K.P.: Systemic and in vitro infection process of *Bombyx mori* nucleopolyhedrovirus. Virus Res. **101**, 109–118 (2004)
12. Torquato, F.B.E., Neto, M.H.D.M., Brancalhäo, R.M.C., Franco, V.S.: Nucleopolyhedrovirus: scanning electron microscopy technique. Neotrop. Entomol. **35**, 787–790 (2006)
13. Adams, J.R., Wilcox, T.A.: Scanning electron microscopical comparisons of insect virus occlusion bodies prepared by several techniques. J. Invertebr. Pathol. **40**, 12–20 (1982)
14. Mündermann, L., Erasmus, Y., Lane B., Coen E., Prusinkiewicz, P.: Quantitative modeling of *Arabidopsis* development. Plant Physiol. **139**, 960–968 (2005)
15. Roose T., Chapman, S.J., Maini, P.K.: Mathematical models of avascular tumor growth. SIAM Rev. **49**, 179–208 (2007)
16. Zayed, J.M., Nouvel, N., Rauwald, U., Scherman, O.A.: Chemical complexity—supramolecular self-assembly of synthetic and biological building blocks in water. Chem. Soc. Rev. **39**, 2806–2816 (2010)